# Interaction Parameters of Carbon in Liquid Iron and the Thermodynamics of Carbon and Oxygen in Alloyed Iron Melts

## K. V. Malyutin and S. N. Paderin

*Moscow State Institute of Steel and Alloys (Technical University), Leninskii pr. 4, Moscow, 119936 Russia*

## INTRODUCTION

The thermodynamic calculations of the decarburization of liquid metal, in particular, the estimation of oxygen distribution for the oxidation of carbon, iron, and other melt components, assume the determination of the carbon and oxygen activities in a metallic solution at given composition and temperature.

For dilute binary solutions of carbon in liquid iron, zero-order ($\ln\gamma_C^\infty$) and first-order ($\varepsilon_C^C$) molar self-interaction parameters are used. In the case of a relatively high carbon concentration, a second-order ($\rho_C^C$) interaction parameter should also be taken into account. The values of the parameters available in reference books [1–3] (published in different years) differ substantially. This makes the use of the data for the calculations difficult. Thus, to increase the accuracy of the calculations, the correct selection of these magnitudes and the determination of their temperature dependences are necessary.

When performing thermodynamic calculations of the carbon activity in alloyed melts, equilibrium oxygen contents should be determined and taken into account along with the concentrations of other components.

## ACTIVITY COEFFICIENT OF CARBON IN AN INFINITELY DILUTE SOLUTION IN LIQUID IRON

The Gibbs energy $\Delta G_C^\infty$ of the reaction of transition of carbon from the standard state "pure substance" into the standard state "hypothetical 1% solution"

$$C_{(graphite)} = [C]_{1\%} \qquad (1)$$

allows the activity coefficient of carbon in an infinitely dilute solution $\gamma_C^\infty$ to be determined by the equation [4]

$$RT\ln\gamma_C^\infty = \Delta G_C^\infty - RT\frac{A_{Fe}}{100A_C}, \qquad (2)$$

where $A_{Fe}$ and $A_C$ are the atomic weights of solvent (iron) and solute (carbon), respectively.

According to [1], the Gibbs energy of reaction (1) is

$$\Delta G_C^\infty = 22600 - 43.2T, \text{ J/mol.} \qquad (3)$$

Equations (2) and (3) can be used to determine the temperature dependence and activity coefficient of carbon in its infinitely dilute solution in liquid iron:

$$\ln\gamma_C^\infty = \frac{2718}{T} - 2.013, \quad \gamma_{C,\,1873\,K}^\infty = 0.57. \qquad (4)$$

In later work [2], the temperature dependence of the Gibbs energy of reaction (1) was refined:

$$\Delta G_C^\infty = 17230 - 39.87T, \text{ J/mol.}$$

This allows us to refine the temperature dependence of $\gamma_C^\infty$:

$$\ln\gamma_C^\infty = \frac{2072}{T} - 1.726, \quad \gamma_{C,\,1873\,K}^\infty = 0.54. \qquad (5)$$

The values of $\gamma_C^\infty$ determined by Eqs. (4) and (5) differ slightly; nevertheless, Eq. (5) is preferable.

## FIRST-ORDER SELF-INTERACTION PARAMETERS OF CARBON IN LIQUID IRON

The temperature dependence of the first-order self-interaction mass parameter of carbon in liquid iron $e_C^C$ and its value at 1873 K are given in [1]:

$$e_C^C = \frac{158}{T} + 0.0581, \quad e_{C,\,1873\,K}^C = 0.143.$$

The conversion of the mass parameter $e_C^C$ into the molar parameter $\varepsilon_C^C$ by the formula

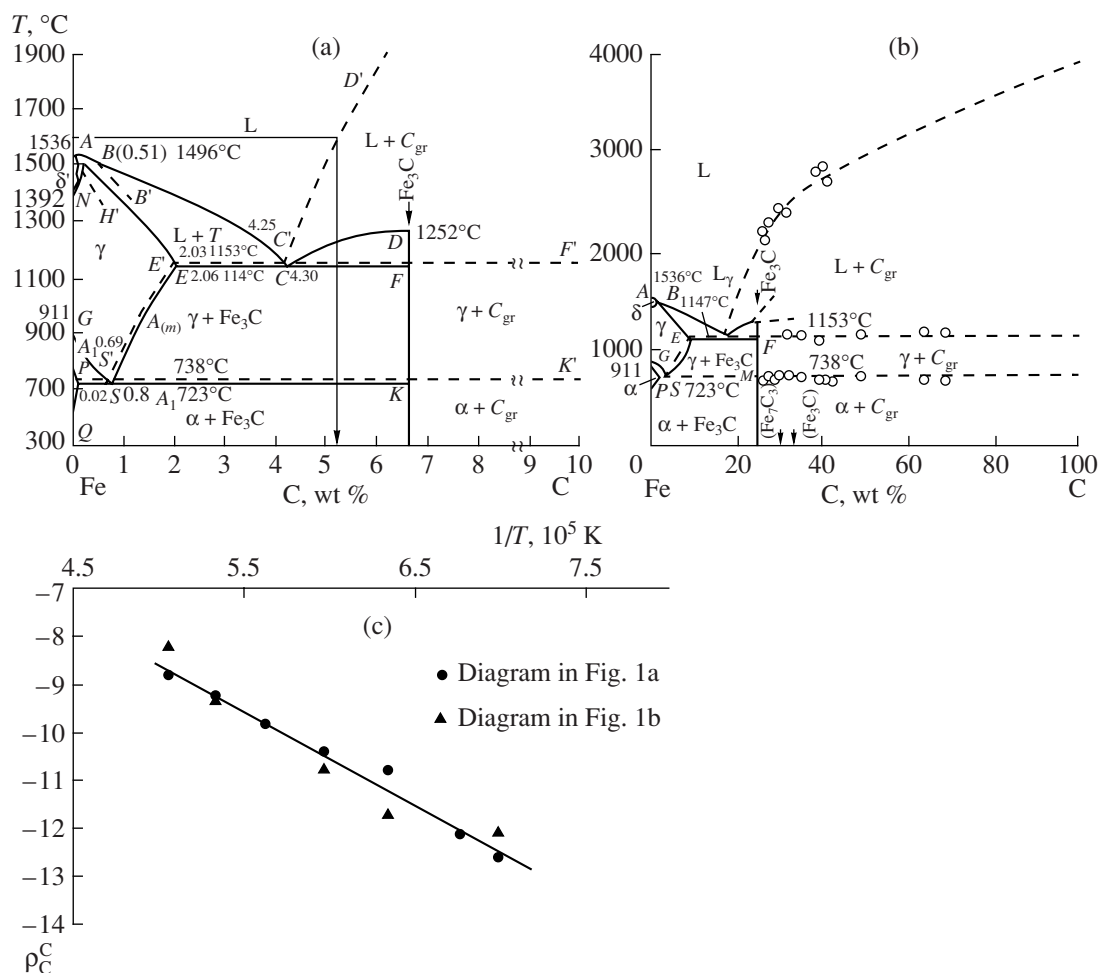$$\varepsilon_C^C = 230\frac{A_C}{A_{Fe}}e_C^C + \frac{A_{Fe} - A_C}{A_{Fe}} \qquad (6)$$

**Fig. 1.** Fe–C phase diagram [5] and the temperature dependence of the parameter $\rho_C^C$ calculated from these two versions of the phase diagram.

gives $\varepsilon_C^C = 7.8$. However, the authors of [1] in [3] recommend using the highest value of this parameter, namely, $\varepsilon_{C,\,1873\,K}^C = 11$.

The conversion into the mass parameter by the formula

$$e_C^C = \frac{1}{230}\frac{A_{Fe}}{A_C}\varepsilon_C^C + \frac{A_C - A_{Fe}}{A_C}$$

gives $e_{C,\,1873\,K}^C = 0.21$.

The refined value of the $e_C^C$ parameter at 1873 K,

$$e_{C,\,1873\,K}^C = 0.243,$$

is given in [2]; however, its temperature dependence is not reported.

The temperature dependence of the $e_C^C$ parameter given in [1] can be used; however, its value at 1873 K should be increased from 0.143 to 0.243. In this case,

the temperature dependence of the $e_C^C$ parameter takes the form

$$e_C^C = \frac{158}{T} + 0.159.$$

Using this dependence in Eq. (6), which is applied to calculate the molar parameter from the mass parameter, we obtain the temperature dependence of the molar parameter of carbon self-interaction:

$$\varepsilon_C^C = \frac{7787}{T} + 8.622, \quad \varepsilon_{C,\,1873\,K}^C = 12.8. \quad (7)$$

## ESTIMATION OF SECOND-ORDER SELF-INTERACTION PARAMETERS OF CARBON IN LIQUID IRON

Let us estimate the second-order interaction parameters of carbon $\rho_C^C$ using two versions of the Fe–C phase diagram (Figs. 1a, 1b) [5]. We assume that, for

**Table 1.** Results of the calculation of the parameter $\rho_C^C$ from the Fe–C phase diagram

| T, K | From the diagram in Fig. 1a | | | From the diagram in Fig. 1b | | $\rho_C^C = \dfrac{-19733}{T} + 1.33$ |
|------|-------------|-------------|-------------|-------------|-------------|---|
| | [C]$_{sat}$, % | $x_C$, sat | $\rho_C^C$ | $x_C$, sat | $\rho_C^C$ | |
| 1426 | 4.25 | 0.171 | −12.62 | 0.17 | −12.08 | −12.51 |
| 1473 | 4.35 | 0.175 | −12.14 | 0.175 | −12.14 | −12.07 |
| 1573 | 4.57 | 0.182 | −10.8 | 0.184 | −11.69 | −11.21 |
| 1673 | 4.79 | 0.190 | −10.37 | 0.191 | −10.77 | −10.46 |
| 1773 | 5.00 | 0.197 | −9.84 | 0.197 | −9.84 | −9.8 |
| 1873 | 5.20 | 0.203 | −9.32 | 0.203 | −9.32 | −9.21 |
| 1973 | 5.37 | 0.209 | −8.83 | 0.207 | −8.19 | −8.67 |

the saturated solution of carbon in liquid iron, the carbon activity at the liquidus is $a_{C, sat} = 1$. In this case,

$$\ln a_{C, sat} = \ln x_{C, sat} + \ln \gamma_{C, sat} = 0,$$

where

$$\ln \gamma_{C, sat} = \ln \gamma_C^\infty + \varepsilon_C^C x_{C, sat} + \rho_C^C (x_{C, sat})^2.$$

From these equations, we can derive an equation for the calculation of the $\rho_C^C$ parameter:

$$\rho_C^C = \frac{-(\ln \gamma_C^\infty + \varepsilon_C^C x_{C, sat} + \ln x_{C, sat})}{(x_{C, sat})^2}. \qquad (8)$$

The parameters calculated for a temperature of 1873 K by Eqs. (5) and (7) are $\ln \gamma_C^\infty = -0.620$ and $\varepsilon_C^C = 12.8$, respectively. According to the phase diagram in Fig. 1a, the point at $T = 1873$ K corresponds to the composition [C] = 5.20% or $x_C = 0.203$. In this case, the parameter calculated by Eq. (8) is $\rho_C^C = -9.32$.

The analogous calculations of the $\rho_C^C$ parameter were performed at other temperatures of the melt, i.e., at 1426–1973 K, using points at the liquidus lines in both versions of the Fe–C phase diagram (Figs. 1a and 1b). Table 1 gives the carbon concentrations corresponding to these points and the calculated values of the $\rho_C^C$ parameter.

According to the dilute solution theory in [6], the temperature dependence of the interaction parameter should take the form $\rho_i^i = \dfrac{a}{T} + b$. The $\rho_C^C$ parameters given in Table 1 adequately fall in a segment of the straight line plotted on the $\rho_C^C$ – $1/T$ coordinates (Fig. 1c). The least squares processing of the data in these coordinates leads to the regression equation

$$\rho_C^C(T) = \frac{-19733}{T} + 1.33 \qquad (9)$$

with a high correlation coefficient ($r = -0.981$).

The values of the $\rho_C^C$ parameter calculated by Eq. (9) (Table 1, the right column) are comparable with those calculated from both versions of the Fe–C phase diagram. We suggest using Eq. (9) for the estimation of the $\rho_C^C$ parameter in a temperature range of 1426–1973 K.

Table 2 lists the self-interaction parameters of carbon in liquid iron and their temperature dependences calculated using reported data and the Fe–C phase diagram in [5].

With the parameters given in Table 2, we can calculate the activity coefficient and activity of carbon in liquid iron at a given concentration:

$$\ln \gamma_C = \ln \gamma_C^\infty + \varepsilon_C^C x_C + \rho_C^C (x_C)^2; \quad a_C = \gamma_C x_C.$$

At a low carbon concentration, the second-order parameter $\rho_C^C$ may be neglected, and the activity coefficient and activity of carbon can be calculated by the equations

$$\ln \gamma_C' = \ln \gamma_C^\infty + \varepsilon_C^C x_C; \quad a_C' = \gamma_C' x_C.$$

**Table 2.** Self-interaction parameters of carbon in liquid iron

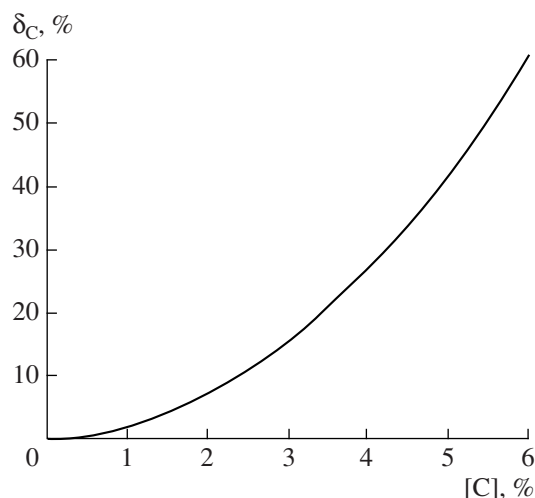| Value at 1873 K | Temperature dependence of the parameter |
|-----------------|------------------------------------------|
| $\gamma_C^\infty = 0.538$ | $\ln \gamma_C^\infty = \dfrac{2072}{T} - 1.726$ |
| $\varepsilon_C^C = 12.8$ | $\varepsilon_C^C = \dfrac{7787}{T} + 8.622$ |
| $\rho_C^C = -9.21$ | $\rho_C^C = \dfrac{-19733}{T} + 1.33$ |

$\delta_C$, %



**Fig. 2.** Relative error of calculating the carbon activity in liquid iron at $T = 1873$ K that is related to the neglect of the $\rho_C^C$ parameter.

The related relative error of the activity calculation is

$$\delta_C = \frac{a_C' - a_C}{a_C} \times 100\%;$$

it increases with the carbon concentration (Fig. 2).

At a carbon concentration [C] = 0.1% in the melt at 1873 K, the relative calculation error is negligible ($\delta_C = 0.02\%$); at [C] = 0.1%, the error is $\delta_C = 1.88\%$. In the saturated solution ([C] = 5.2%), the error reaches 45%.

When calculating the carbon activity in liquid iron with a carbon content higher then 1%, it is reasonable to use the parameter $\rho_C^C$.

## CARBON AND OXYGEN ACTIVITIES IN AN ALLOYED STEEL

At present, an innovative (vacuum) technology for deep decarburization of alloyed melts in complex out-of-furnace treatment plants is being implemented at high-quality metallurgical works [7]. In connection with the use of such innovative technologies, it is a challenge to analyze changes in the carbon and oxygen activities, from the onset of the oxidation process at a sufficiently high carbon concentration (0.40–0.70%), to the end of the process, when the weight fraction of carbon decreases to several hundredths of a percent. We calculated the activity coefficients and activities of carbon and oxygen for five pilot heats of a corrosion-resistant steel, which differed in metal composition and the temperature at the beginning and end of an oxidation process in a vacuum (Table 3). The partial pressure of CO in gas bubbles during metal boiling was taken to be $p_{CO} = 0.1$. The principal contribution to this value was made by the ferrostatic pressure of the metal at an effec-

tive boiling depth $h \approx 15$ cm. When calculating, we took into account the effect of alloying components (chromium, nickel), the residual silicon and manganese contents, and the equilibrium oxygen content.

We used the reaction of carbon oxidation at 1500–2000 K,

$$C_{(graphite)} + 1/2 O_{2(g)} = CO_{(g)},$$
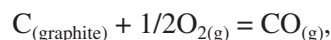
$$\Delta G^0 = -114\,515 - 86.015T,\ \frac{J}{mol},$$

whose equilibrium constant is

$$K = \frac{p_{CO}}{a_C a_O} = \frac{0.1}{x_C x_O \gamma_C \gamma_O} = e^{\frac{\Delta G^0}{RT}}.$$

At given temperature and carbon concentration $x_C$, the carbon activity and equilibrium oxygen concentration are

$$a_C = \gamma_C x_C; \quad x_O = \frac{0.1}{K x_O \gamma_C \gamma_O}. \tag{10}$$

The activity coefficients of carbon $\gamma_C$ and oxygen $\gamma_O$ are expressed in terms of interaction parameters $\varepsilon_i^j$:

$$\ln \gamma_C = \ln \gamma_C^\infty + \varepsilon_C^C x_C + \varepsilon_C^O x_O + \varepsilon_C^{Cr} x_{Cr}$$
$$+ \varepsilon_C^{Ni} x_{Ni} + \varepsilon_C^{Mn} x_{Mn} + \varepsilon_C^{Si} x_{Si}, \tag{11}$$

$$\ln \gamma_O = \ln \gamma_O^\infty + \varepsilon_O^O x_O + \varepsilon_O^C x_C + \varepsilon_O^{Cr} x_{Cr}$$
$$+ \varepsilon_O^{Ni} x_{Ni} + \varepsilon_O^{Mn} x_{Mn} + \varepsilon_O^{Si} x_{Si}, \tag{12}$$

where

$$\ln \gamma_C^\infty = \frac{2072}{T} - 1.726, \quad \gamma_{C,\,1873\,K}^\infty = 0.538,$$

$$\ln \gamma_O^\infty = -\frac{14424}{T} + 3.275, \quad \gamma_{O,\,1873\,K}^\infty = 0.012,$$

$$\varepsilon_C^C = \frac{7787}{T} + 8.622, \quad \varepsilon_O^O = -\frac{115000}{T} + 50.66.$$

The interaction parameters at $T = 1873$ K [2] are as follows:

|  | C | O | Cr | Ni | Mn | Si |
|---|---|---|---|---|---|---|
| $\varepsilon_C^i$ | 12.8 | −20 | −2.0 | 2.37 | −1.88 | 9.75 |
| $\varepsilon_O^i$ | −20 | −10.7 | −4.84 | 2.40 | −4.7 | −7.10 |

At other temperatures, the parameters of interaction of carbon and oxygen with alloying components were corrected by the equation

$$\varepsilon_{i,\,T}^j = \varepsilon_{i,\,1873\,K}^j \frac{1873}{T}.$$

The calculation, according to the system of Eqs. (10)–(12), is difficult owing to the fact that, to cal-

**Table 3.** Compositions of alloyed melts upon vacuum decarburization in a 10-t unit and the activity coefficients of carbon and oxygen calculated for these compositions

| Heat | Steel grade | Element | At the beginning of the oxidation process under vacuum | | | | | | At the end of the oxidation process under vacuum | | | | | |
|---|---|---|---|---|---|---|---|---|---|---|---|---|---|---|
| | | | C | Si | Mn | Cr | Ni | O | C | Si | Mn | Cr | Ni | O |
| 1 | 12Kh18N10T | | | | | *T* = 1913 K | | | | | | *T* = 1968 K | | |
| | | $\%i$ | 0.70 | 0.21 | 1.52 | 18.90 | 10.21 | UM* | 0.04 | 0.02 | 1.05 | 18.58 | 10.41 | UM |
| | | $x_i$ | 0.0314 | 0.00403 | 0.0149 | 0.196 | 0.0937 | $4.44 \times 10^{-4}$ | 0.00184 | 0.000394 | 0.0106 | 0.198 | 0.0980 | 0.00209 |
| | | $\gamma_i$ | 0.381 | | | | | $4.49 \times 10^{-4}$ | 0.244 | | | | | 0.00157 |
| | | $a_i$ | 0.00120 | | | | | $1.99 \times 10^{-7}$ | 0.000449 | | | | | $6.48 \times 10^{-6}$ |
| 2 | 12Kh18N10T | | | | | *T* = 1852 K | | | | | | *T* = 1964 K | | |
| | | $\%i$ | 0.52 | 0.15 | 1.52 | 17.31 | 9.93 | UM | 0.03 | 0.02 | 1.07 | 16.92 | 10.54 | UM |
| | | $x_i$ | 0.0235 | 0.00290 | 0.0150 | 0.181 | 0.0918 | $4.34 \times 10^{-4}$ | 0.00092 | 0.00039 | 0.00757 | 0.180 | 0.0994 | 0.00408 |
| | | $\gamma_i$ | 0.357 | | | | | $5.17 \times 10^{-4}$ | 0.263 | | | | | 0.00194 |
| | | $a_i$ | 0.00839 | | | | | $2.24 \times 10^{-7}$ | 0.000364 | | | | | $7.89 \times 10^{-6}$ |
| 3 | 08Kh17T | | | | | *T* = 1885 K | | | | | | *T* = 2003 K | | |
| | | $\%i$ | 0.54 | 0.10 | 0.32 | 17.40 | 0.35 | UM | 0.04 | 0.02 | 0.13 | 15.70 | 0.33 | UM |
| | | $x_i$ | 0.0243 | 0.00192 | 0.00315 | 0.181 | 0.00322 | $4.59 \times 10^{-4}$ | 0.00184 | 0.000393 | 0.00130 | 0.166 | 0.00310 | 0.00357 |
| | | $\gamma_i$ | 0.302 | | | | | $6.37 \times 10^{-4}$ | 0.238 | | | | | 0.00211 |
| | | $a_i$ | 0.00733 | | | | | $2.92 \times 10^{-7}$ | 0.000438 | | | | | $7.55 \times 10^{-6}$ |
| 4 | 08Kh17T | | | | | *T* = 1933 K | | | | | | *T* = 2014 K | | |
| | | $\%i$ | 0.42 | 0.09 | 0.52 | 17.34 | 0.36 | UM | 0.02 | 0.01 | 0.33 | 16.08 | 0.6 | UM |
| | | $x_i$ | 0.0190 | 0.00174 | 0.00514 | 0.181 | 0.00333 | $5.65 \times 10^{-4}$ | 0.000918 | 0.000196 | 0.00331 | 0.171 | 0.00564 | 0.00830 |
| | | $\gamma_i$ | 0.286 | | | | | $8.38 \times 10^{-4}$ | 0.213 | | | | | 0.00210 |
| | | $a_i$ | 0.00543 | | | | | $4.73 \times 10^{-7}$ | 0.000195 | | | | | $17.5 \times 10^{-6}$ |
| 5 | 12Kh18N10T | | | | | *T* = 1977 K | | | | | | *T* = 1943 K | | |
| | | $\%i$ | 0.54 | 0.10 | 1.48 | 18.94 | 10.31 | UM | 0.04 | 0.5 | 0.92 | 16.88 | 10.51 | UM |
| | | $x_i$ | 0.0239 | 0.00193 | 0.0146 | 0.198 | 0.0953 | $5.46 \times 10^{-4}$ | 0.00183 | 0.00981 | 0.00922 | 0.179 | 0.0986 | 0.00275 |
| | | $\gamma_i$ | 0.346 | | | | | $6.65 \times 10^{-4}$ | 0.297 | | | | | 0.00178 |
| | | $a_i$ | 0.00829 | | | | | $3.63 \times 10^{-7}$ | 0.000544 | | | | | $4.89 \times 10^{-6}$ |

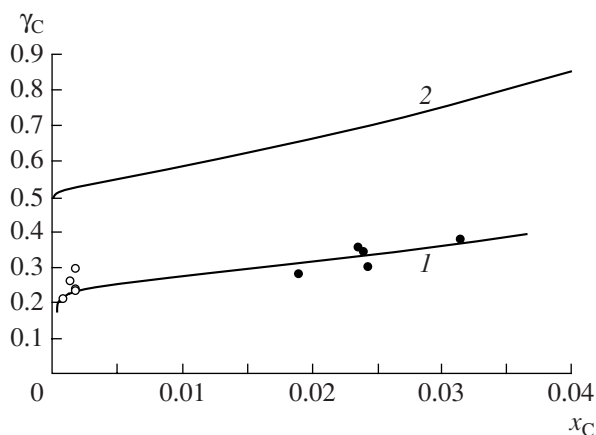* UM means ummeasured.

**Fig. 3.** ($1$) Dependence of the activity coefficient of carbon $\gamma_C$ on its molar fraction $x_C$ for the averaged composition of an alloyed melt and ($2$) the equilibrium curve for an Fe–O–C melt. Points in the curve correspond to the activity coefficients of carbon $\gamma_C$ in the alloyed melts of each heat calculated from the metal composition and temperature.
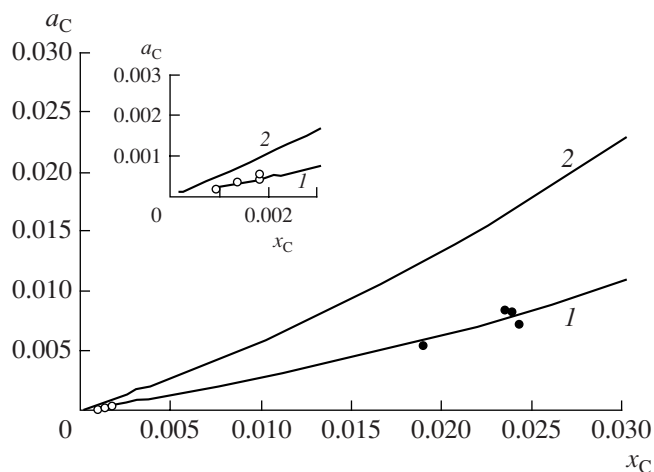


**Fig. 4.** Dependence of the activity of carbon on its molar fraction for the averaged compositions of ($1$) alloyed and ($2$) Fe–O–C melts. Points in the curve correspond to the activity of carbon in the alloyed melts of each heat calculated from the metal composition and temperature.
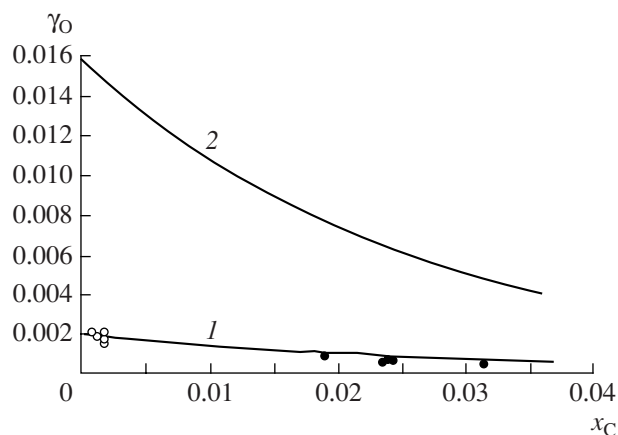


**Fig. 5.** Dependence of the activity coefficient of oxygen $\gamma_O$ on the molar fraction for carbon for the averaged compositions of ($1$) alloyed and ($2$) Fe–O–C melts. Points in the curve correspond to the activity coefficient of oxygen in the alloyed melts of each heat calculated from the metal composition and temperature.
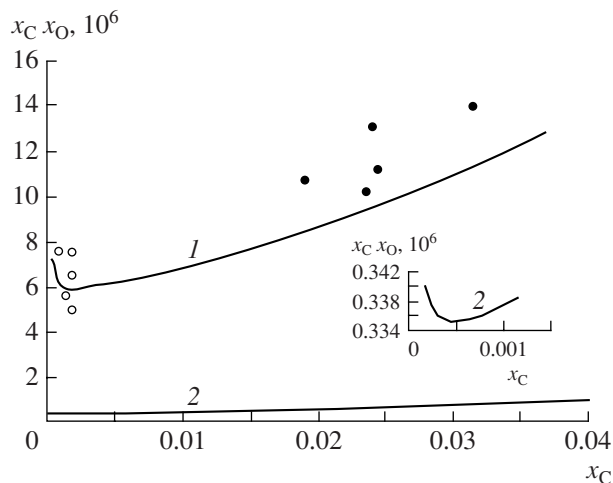


**Fig. 6.** ($1$) Dependence of the product of the molar fractions of oxygen and carbon on the carbon molar fraction for the averaged composition of an alloyed melt and ($2$) the equilibrium curve for an Fe–O–C melt. Points in the curve correspond to the product of the molar fractions of oxygen and carbon in the alloyed melts of each heat calculated from the metal composition and temperature.

culate $a_C$ and $x_O$ by Eq. (10), $x_O$ in Eqs. (11) and (12) must be available. That is why we used the method of successive approximations.

The activity coefficients and activities of carbon and oxygen were calculated using the alloying component contents in the melt averaged over five heats (17.41% Cr, 6.355% Ni, and 0.89% Mn) and the alloying component contents in the Fe–C–O melt at an average temperature of 1945 K. The calculations were performed using the Microsoft Excel 2002 software package.

The initial data, the calculated activity coefficients and activities of carbon, and the equilibrium values of $\gamma_O$, $x_O$, and $a_O$ for oxygen are given in Table 3. Figures 3, 4, 5, and 6 illustrate the calculation results. The calculation of the equilibrium curves of the quantities for the average composition was performed to achieve the minimum molar fraction of carbon, which corresponds to the maximum equilibrium solubility of oxygen. For the alloyed melt, $x_{C,\,min} = 0.00093$; for the Fe–C–O solution, $x_{C,\,min} = 0.000049$.

As is seen from Fig. 6, the product of the molar fractions of carbon and oxygen $x_C \cdot x_O$ in the alloyed melt is located substantially higher than that for the iron–carbon melt. The existence of a minimum in the product of the molar fractions of carbon and oxygen, which was found by Filippov on experimentally studied iron–carbon melts [8], is confirmed by the thermodynamic calculations. In the presence of alloying elements, the value of the minimum increases and it shifts toward high carbon concentrations.

The low activity coefficients $\gamma_C$ and $\gamma_O$ in alloyed melts as compared to those in iron–carbon melts lead to a decrease in the activities of carbon and oxygen in the alloyed melts.

Alloying components such as chromium and manganese are shown to hinder deep decarburization of alloyed melts. However, the use of vacuum during decarburization allows a carbon concentration of 0.02–0.04% to be reached in melts containing 17–18% Cr at the end of the oxidation stage.

## REFERENCES

1. G. K. Sigworth and J. F. Elliot, Metal Science **8**, 298–310; **13**, 445–461 (1974).
2. *Steelmaking Data Source Book* (Gordon & Breach, New York, 1988).
3. J. F. Elliot, R. Gleizer, and V. Ramakrishna, *Theory of Steelkaing Processes* (Metallurgiya, Moscow, 1969) [in Russian].
4. S. N. Paderin and V. V. Filippov, *Theory and Calculations of Metallurgical Systems and Processes* (MISiS, Moscow, 2002) [in Russian].
5. *Phase Diagrams of Binary and Multicomponent Iron-Based Systems: a Handbook*, Ed. by O. A. Bannykh and M. E. Drits (Metallurgiya, Moscow, 1986) [in Russian].
6. K. Lyupis, *Chemical Thermodynamics* (Metallurgiya, Moscow, 1989) [in Russian].
7. S. L. Paren'kov, K. L. Kosyrev, and S. N. Paderin, "On the Way to High Technologies in Steelmaking at the Serp i Molot Plant," Electrometallurgiya, No. 8, 18–25 (2005).
8. S. I. Filippov, *Theory of Steel Decarburization* (Metallurgiya, Moscow, 1966) [in Russian].